26th International Congress of Mechanical Engineering
COBEM 2021
November 22-26, 2021, Virtual Congress, Brazil

COB-2021-0547
MODELING AND COMPUTATIONAL SIMULATION OF VAPOR COMPRESSION REFRIGERATION SYSTEMS IN THE *QUASI*-STEADY STATE REGIME

Leonardo Cavalheiro Martinez
Federal University of Paraná (UFPR) – Graduate Program in Mechanical Engineering (PG-Mec), Coronel Francisco Heráclito dos Santos Avenue, 100 – Jardim das Américas, Curitiba – PR – Brazil
Department of Mechanical Engineering – Pontifical Catholic University of Paraná (PUCPR), Imaculada Conceição St., 1155 – Prado Velho, Curitiba – PR – Brazil
leonardo.cmartinez@live.com

Wellington Balmant
Flávio Junior Santiago Silva
Lauber de Souza Martins
José Viriato Coelho Vargas
Federal University of Paraná (UFPR) – Graduate Program in Mechanical Engineering (PG-Mec), Coronel Francisco Heráclito dos Santos Avenue, 100 – Jardim das Américas, Curitiba – PR – Brazil
wbalmant@gmail.com, flaviojrsantiago@gmail.com, laubermartisn@gmail.com and vargasjvcv@gmail.com

Abstract. Considering the growing energy demand and the increasingly significant use of HVAC-R equipment around the world, the development of new and efficient Vapor Compression Refrigeration Systems (VCRS) becomes an excellent alternative for minimizing this issue. One of the most effective ways to address this is through the conception of mathematical models that can predict the physical behavior of these VCRS. Therefore, in this study, a mathematical model was developed to simulate the *quasi*-steady state physical behavior of a Vapor Compression Cycle (VCC), considering its interaction with the refrigerated space. The mathematical modeling was individually developed for each VCC component operating in steady-state regime, then, all equations were coupled together to simulate the integrated system. The refrigerated space model, on the other hand, was based on the application of the mass and energy (the first law of thermodynamics for control volume) conservation laws and was considered a transient operation, i.e., obtaining the temperature behavior of the refrigerated space over time. This study also proposed an exergy analysis for the vapor compression cycle. This mathematical model was fully implemented with FORTRAN® language; it was able to predict the heat transfer rates involved in the evaporator, the pressure levels on the heat exchangers, the Coefficient of Performance (COP), the second law efficiency, and also, the thermal behavior of the refrigerated space, such as obtaining the pull-down time. Therefore, it is expected that the mathematical model developed in this study can be used for design, simulation, and control of VCC procedures, especially those that involve determining the first and second law efficiencies and also the assessment of the pull-down time for future thermodynamic optimization procedures.

Keywords: *Mathematical Modeling. Computational Simulation. Vapor Compression Cycle. Refrigeration Systems. Pull-Down Time.*

1. INTRODUCTION

According to the latest Brazilian Energy Balance (BEN) released by the Ministry of Mines and Energy (MME), the industrial sector was responsible for approximately 36.6% of Brazil's energy consumption in 2020, followed by residential (27.6%) and commercial (15.7%) ones. If these three sectors are put together, they account for almost 80% of all the electricity consumed in the country (Brazil MME, 2021). In these sectors, refrigeration systems account for a significant portion of the total energy consumption. In any of these sectors, whether industrial, residential, and/or commercial, a significant portion of total energy consumption in several countries around the world is allocated to the operation of heating, ventilation, air conditioning, and refrigeration (HVAC-R) equipment, which comprise HVAC-R operations (Shahrestani *et al.* (2018)). In general, in the industrial, residential, and commercial sectors, the consumption of energy through HVAC-R equipment around the world is 52% (Hu, Wu and Wang (2018)), 47% (Jung and Jazizadeh (2019)), and 40% (Rismanchi *et al*. (2019)), respectively. Using this information, we can verify that approximately 38.3% of the total energy consumption in Brazil is allocated to the most diverse and distinct HVAC-R systems.

Thus, any technological and scientific development aimed at reducing the consumption of electrical energy by HVAC-R equipment will be considered a unique contribution to the world's energy demand. A solution that presents itself as an alternative way to obtain the reduction of energy consumption in HVAC-R systems is the development of mathematical models and the simulation and optimization of the processes. In general, the HVAC-R systems that use the operating principles through the Vapor Compression Cycles (VCC) are the most used nowadays due to their range of applicability in several countries around the world. Considering these aspects, we notice that there are several studies in the scientific literature that aim to contribute to the modeling and simulation of HVAC-R systems area. Some examples are: Zubair *et al.* (2001) proposed a mathematical model based on Finite Difference Equations (FDE) to evaluate the ideal performance, through COP, of four HVAC-R systems through adequate distribution of the total thermal exchange area between the systems' evaporator and condenser. Wang *et al.* (2007) developed a mathematical model with experimental validation to analyze the spatial distribution of the refrigerant fluid inside the heat exchangers of a VCC and, consequently, calculate the two-phase region (liquid and gas) of the evaporator and condenser by checking a velocity gradient. Nunes *et al.* (2015) presented a simplified dimensionless mathematical model for a Vapor Compression Refrigeration System operated in transient regime aiming at optimizing the dynamic response of the system. In 2017, Yang, Ordoñez, and Vargas presented a steady-state mathematical model and a structured methodology to optimize the internal structure (heat exchanger areas) and the pressure ratio of a vapor compression refrigeration system; to do that, the refrigeration rate, COP, and second law efficiency were maximized. Finally, in 2019, Hermes evaluated the influence of the insertion of an Internal Heat Exchanger (IHE) in a Vapor Compression Cycle operating in a steady-state regime on the evaporator cooling effect on the refrigerant fluid volume at the compressor inlet and on the power of compression, as well as the suction line pressure drop, i.e., for the study developed by the author, between the evaporator and the Internal Heat Exchanger (IHE) itself.

Considering the technical works and scientific studies presented above, is possible to define this study's purpose as the development of a mathematical model to simulate the *quasi*-steady-state physical behavior of a VCC, considering its interaction with the refrigerated space. The model is fully implemented using Fortran® 95 language. The equations that govern the mathematical model are based in the mass and energy conservation laws.

2. MATHEMATICAL MODEL

The mathematical model in steady-state regime for each component that make up the VCC (compressor, condenser, expansion valve, and evaporator) is described below, as well as the transient modeling for the refrigerated space. For this, it will be considered the representative scheme that is shown in Figure 01. The steady-state model for the refrigeration system used in this study is based on Yang, Ordoñez and Vargas (2017).

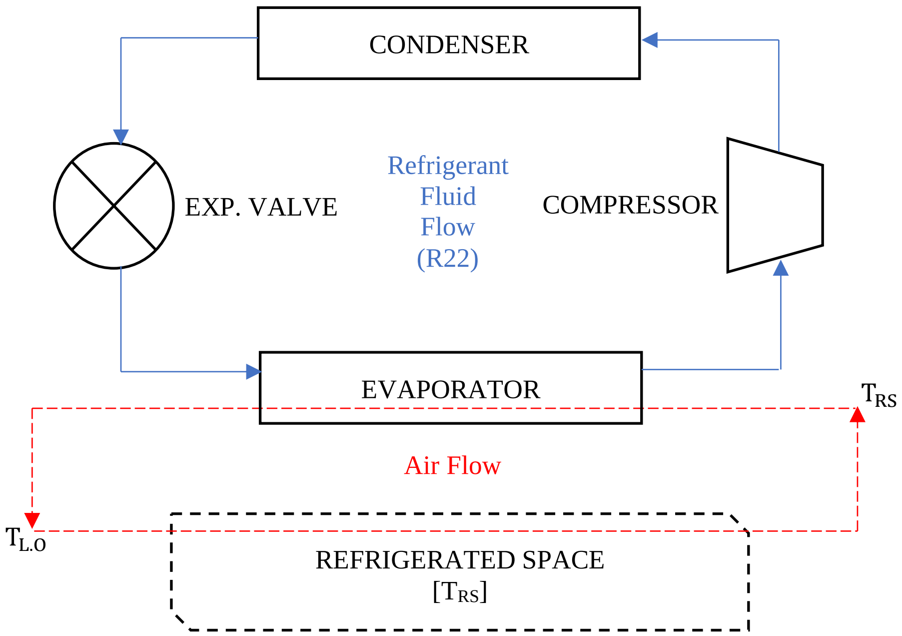

Figure 01. Representative Scheme of a VCC.

The physical system was divided in one control volume for each analysis region: one control volume for the VCC and another control volume for the Refrigerated Space (RS), specifically. As already mentioned in Section 1, the model presented in this study is based on the application of the mass and energy conservation laws, ignoring the influence of the potential and kinetics energies, and also considering that the total energy of a VCC's component is present only as Internal Energy.

2.1 Vapor Compression Cycle in Steady State

VCC is composed of four components, as presented in Figure 01: compressor, condenser, expansion valve, and evaporator. The mathematical model presented for the VCC was based on what is sought in this study and was developed in steady state.

2.1.1 Evaporator and Condenser Pressures

Considering that the compression in the compressor occurs according to a polytropic process, an equation to obtain the compressor power can be defined [Yang, Ordoñez and Vargas, 2017].

$$\dot{W}_{CP} = \frac{n}{1-n}\eta_V V_S \omega_{CP} p_{EVAP}\left\{1-\left(\frac{p_{COND}}{p_{EVAP}}\right)^{(n-1)/n}\right\}\sigma_{CP} \tag{01}$$

where the V_S term represents the compressor swept volume [m³] and ω_{CP} corresponds to the compressor angular velocity [RPS]. The terms p_{COND} and p_{EVAP} denote, respectively, the condenser and evaporator pressures [Pa], n refers to the polytropic coefficient of the compression process [-] and σ_{CP} is a dimensionless quantity defined as the isentropic coefficient of the compressor suction [-]. In addition, the volumetric efficiency of the VCC's compressor, represented by η_V [-], is defined as:

$$\eta_V = 1 + \chi - \chi\left(\frac{p_{COND}}{p_{EVAP}}\right)^{1/n} \tag{02}$$

where χ corresponds to the dead volume ratio [-], given by $\chi = V_D/V_S$ and V_D representing the dead volume of the compressor [m³].

As the compressor power is a known parameter in this study, the evaporator and condenser pressures can be calculated via Eq. (01) and (02).

2.1.2 Coefficient of Performance

The Coefficient of Performance (COP), treated as a figure of merit for a refrigeration system, is obtained by the ratio between the desired effect with the cycle [$\dot{Q}_{EVAP}$, W] and the energy input [$\dot{W}_{CP}$, W], such as:

$$COP_{VCC} = \frac{\dot{Q}_{EVAP}}{\dot{W}_{CP}} \tag{03}$$

where:

$$\dot{Q}_{EVAP} = \dot{m}_{AIR} c_{p,AIR}\left(T_{L,O} - T_{RS}\right) \tag{04}$$

where $\dot{m}_{AIR}$ denotes the air mass flow through the evaporator [kg.s^{-1}] and T_{RS} is the temperature of the refrigerated space when it reaches the steady state [K]. $c_{p,AIR}$ represent the specific heat at constant pressure [J.kg^{-1}.K^{-1}]. This information is obtained for the air in the evaporator. Besides, $T_{L,O}$ represents the temperature of the air at the evaporator outlet [K], estimated by:

$$T_{L,O} = -0.0008\, T_{RS}^3 + 0.7204\, T_{RS}^2 - 220.24\, T_{RS} + 22647 \tag{05}$$

Eq. (05), represented by the third-degree polynomial of the temperature of the air at the evaporator outlet ($T_{L,O}$) as a function of T_{RS}, was obtained by simulating a mathematical model that considers the relationship between the refrigeration system and its refrigerated space. The model used for this simulation of the refrigeration system has a high degree of complexity and, among other features, considers the superheating and subcooling regions of the refrigerant fluid, as well as analyses the head losses involved in the heat exchangers (condenser and evaporator) of the system. This model, as already stated in Section 2, is fully simulated on a steady-state basis considering R22 as refrigerant fluid and is presented in the study developed by Yang, Ordoñez, and Vargas (2017). Therefore, it is possible to state that a stationary model for the refrigeration system is available.

As seen in Figure 02, the refrigerated space, unlike the refrigeration system, is modeled and simulated in a transient regime, which, after the solutions, provides the T_{RS} value for insertion into the refrigeration system model, along with the air mass flow rate, but that is treated as a fixed simulation parameter in this study. In return, the refrigeration system model can provide what $T_{L,O}$ will be. Thus, for different values of T_{RS} that are imputed to the refrigeration system model, it is possible to obtain the various values for $T_{L,O}$, and to observe that $T_{L,O}$ depends only on T_{RS}, as the air mass flow rate is kept fixed (Figure 03).

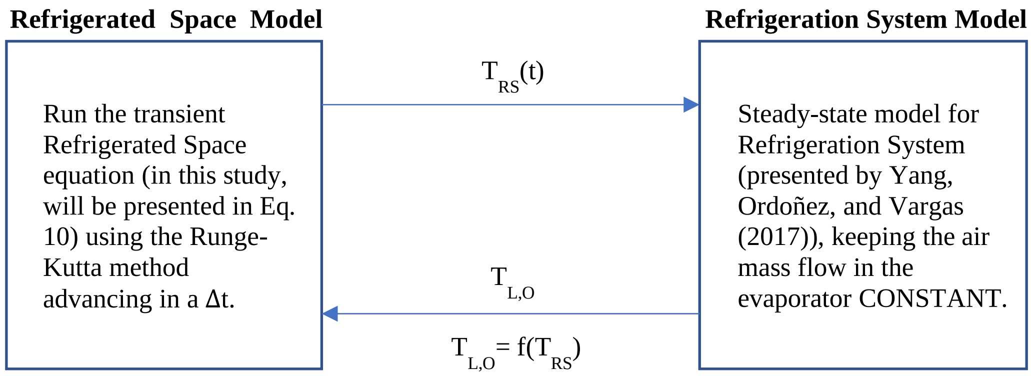

Figure 02. Relationship between the Refrigeration System and Refrigerated Space.

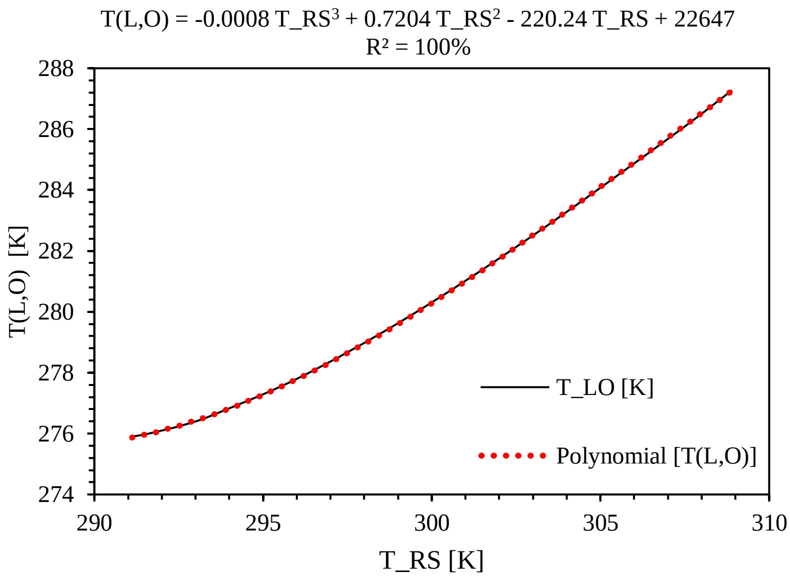

Figure 03. $T_{L,O}$ depending on T_{RS}.

This approach allows for a reduction in time and computational effort, as it is not necessary to simulate the refrigeration system model at each step in which the transient model of the refrigerated space is being solved. However, the interaction and effect of the refrigeration system itself is still observed in obtaining T_{RS}.

Alternatively, the heat transfer rate that the evaporator needs to withdraw from the refrigerated space [$\dot{Q}^*_{EVAP}$, W] can be calculated considering the effect of heat transfer with the external environment and also the intensity of thermal load [$\dot{Q}_{GEN}$, W]:

$$\dot{Q}^*_{EVAP} = \dot{Q}_{GEN} + \dot{Q}_\infty = \dot{Q}_{GEN} + UA(T_\infty - T_{RS}) \tag{06}$$

where U represents the global heat transfer coefficient [$W.m^{-2}.K^{-1}$] and A denotes the heat transfer area of the refrigerated space [m^2].

Another analysis can be done by calculating COP considering the heat transfer in the evaporator obtained through Eq. (06), called COP_{SYSTEM}, since it is intended to obtain the Coefficient of Performance for the system in steady-state regime:

$$COP_{SYSTEM} = \frac{\dot{Q}^*_{EVAP}}{\dot{W}_{CP}} \tag{07}$$

2.1.3 2nd Law Efficiency

The second law efficiency for the refrigeration cycle between 0 and 100% can be defined by the actual exergy input rate [$-\dot{E}_{Qevap}$, W] divided by the ratio of the minimum exergy rate (power) requirement [$\dot{W}_{CP}$, W] (Yang, Ordoñez and Vargas, 2017), given by:

$$\eta_{II} = \frac{-\dot{E}_{Qevap}}{\dot{W}_{CP}} \tag{08}$$

where $-\dot{E}_{Qevap}$ is defined by an exergy balance on the air side, that is treated as an ideal gas, which flows into the evaporator:

$$-\dot{E}_{Qevap} = \dot{m}_{AIR} c_{p,AIR} \left[\left(T_{L,O} - T_{RS} \right) - \ln\left(\frac{T_{L,O}}{T_{RS}} \right) \right] \tag{09}$$

2.2 Refrigerated Space

In order to develop the mathematical model that represents the temporal distribution of the refrigerated space temperature [dT_{RS}/dt, K.s^{-1}], thermodynamic properties [$c_{v,AIR}$, J.kg^{-1}.K^{-1}] are considered uniform and the air mass in refrigerated space [m_{AIR}, kg] is treated as constant. The effects of $\dot{Q}_\infty$ and $\dot{Q}_{GEN}$ are also considered. Based on mass and energy conservation principles considering the transient regime for the refrigerated space:

$$\frac{dT_{RS}}{dt} = \frac{1}{m_{AIR} c_{v,AIR}} \left\{ \dot{Q}_{GEN} + \dot{Q}_\infty + \dot{m}_{AIR} c_{p,AIR} \left(T_{L,O} - T_{RS} \right) \right\} \tag{10}$$

Eq. (10) allows us to obtain the thermal behavior of the refrigerated space and, therefore, analyzing the pull-down time, which is the time required for the system to leave an initial temperature and reach the steady-state condition (Yang and Yeh, 2015). Although it is possible to replace Eq. (05) inside Eq. (10) and integrate this Ordinary Differential Equation (ODE) through the separation of variables method to obtain an analytical solution of $T_{RS}(t)$, this solution is not simple, therefore, in this study the authors chose to consider the mathematical model with the differential behavior shown in Eq. (10).

2.3 Numerical Parameters and Simulation's Configuration

The mathematical model for the VCC described in Sections 2.1 and 2.2 was implemented using FORTRAN® 95 language admitting R22 as the refrigerant fluid. All simulations were performed in an Intel (R) Core (TM) i7-8565U CPU @ 1.80 GHz, 8 GB RAM and 64-bit operating system laptop. In order to obtain numerical answers with it, it was necessary to define a set of input parameters that are shown in Table 01. The input data was selected for a VCC system base configuration with an appropriate environmental, geometric, and operating condition for the studied case.

Table 01. Numerical Parameters for the VCC and Refrigerated Space Simulation.

$\dot{W}_{CP}$ [kW]	1.5
n [-]	1.2
χ [-]	0.05
V_S [m³]	$115 \cdot 10^{-6}$
ω_{CP} [RPS]	42
σ_{CP} [-]	0.808
$p_R = p_{COND}/p_{EVAP}$ [-]	6
$\dot{m}_{AIR}$ [kg.s^{-1}]	0.2
$c_{p,AIR}$ [kJ.kg^{-1}.K^{-1}]	1.005
$c_{v,AIR}$ [kJ.kg^{-1}.K^{-1}]	0.716
U [kW.m^{-2}.K^{-1}]	0.001472
A [m²]	54
T_∞ [K]	298.15
m_{AIR} [kg]	27

As Eq. (10), presented in Section 2.2, is an Ordinary Differential Equation (ODE), it was solved using the fixed step Runge-Kutta method of 4th-5th order over time with an initial condition for T_{RS} equal to 330,15 K and considering several thermal loads ($\dot{Q}_{GEN}$). In addition, it is important to mention that the fixed step considered for the solution was 10s and the maximum simulation time was fixed at 1500s, since, at this time, the steady state for the refrigerated space was already reached. Each time that a T_{RS} temperature was obtained, it was directed to the model described in Section 2.1 and, with that, the answers were obtained in the steady state. Every time that a complete solution cycle of the VCC and refrigerated space is obtained, a new solution step is added.

3. RESULTS AND DISCUSSION

The mathematical model developed in Section 2 is used in this study to produce results in order: (i) to investigate a transient response for the behavior of air temperature in the refrigerated space under several thermal load conditions, (ii) to observe the physical behavior of COP and second law efficiency as a function of thermal load variation, and (iii) to obtain the pressure levels of the refrigerant fluid that flows inside of the heat exchangers (e.g., condenser and evaporator). To obtain results, different values were simulated for the thermal load that is present inside the refrigerated space: 0.75 kW, 1.00 kW, 1.50 kW, 2.00 kW, 2.50 kW, 2.60 kW, 2.70 kW, 2.80 kW, 2.90 kW, 3.00 kW, 3.50 kW, 4.00 kW, 4.50 kW, 5.00 kW, and 5.20 kW.

Figure 04 shows the physical behavior of the air temperature inside the refrigerated space for some thermal load values: 0.75 kW, 1.50 kW, 2.50 kW, 3.00 kW, 4.00 kW and 5.00 kW. The thermal load values selected to be presented in Figure 04 refer to those that, graphically, presented a better visual quality so that the pull-down time was clearly shown. Both Figure 04 and in Table 02 (for all thermal load values) show that the pull-down time is greater, the greater the thermal load installed inside the refrigerated space. This is because when the thermal load ($\dot{Q}_{GEN}$) is low, the refrigeration system only needs to be responsible for removing heat from the external environment ($\dot{Q}_{\infty}$). Another fact that can be seen is that the lower the thermal charge intensity, the lower the temperature reached inside the refrigerated space.

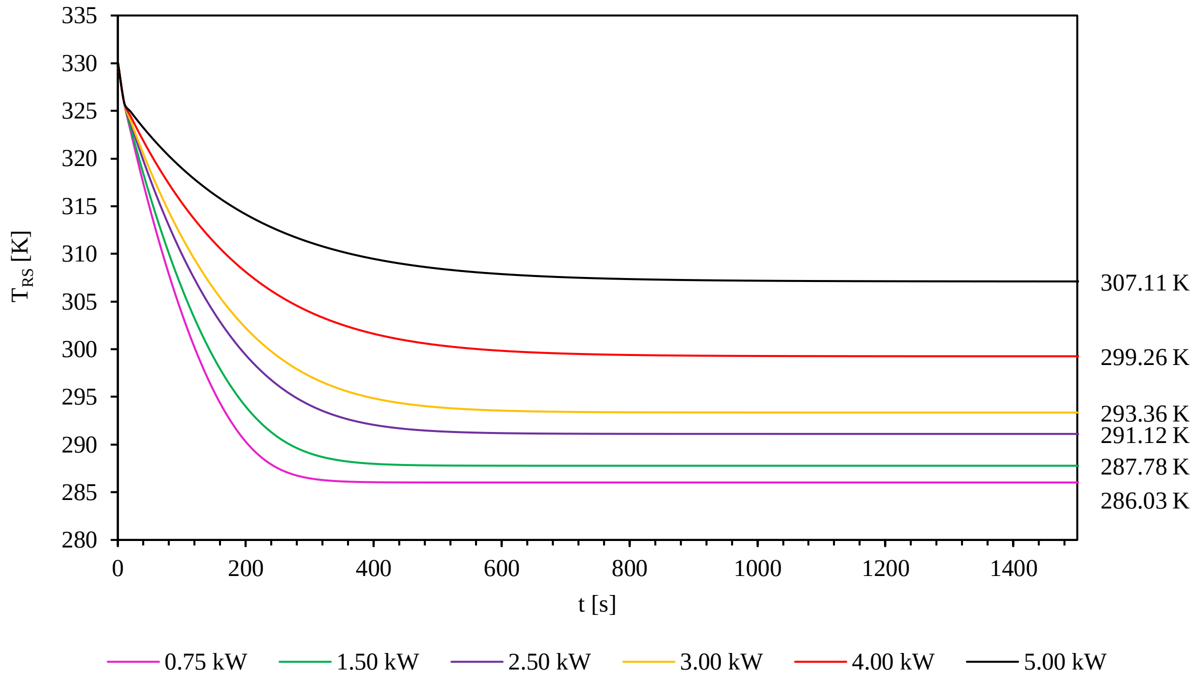

Figure 04. Temperature Distribution of the Refrigerated Space over time (Pull-Down Time) for some Thermal Loads.

Table 02. Pull-Down Time obtained on Refrigerated Space.

$\dot{Q}_{GEN}$ [kW]	t_{PD} [s]
0.75	450
1.00	590
1.50	610
2.00	730
2.50	820
2.60	840

2.70	860
2.80	880
2.90	910
3.00	1000
3.50	1270
4.00	1310
4.50	1350
5.00	1390
5.20	1400

Figures 05 and 06 show, respectively, COP profile and the second law efficiency in relation to the thermal load values. Figure 05 shows that for the $\dot{Q}_{GEN}$ values tested in this study, the COP_{VCC} tends to increase as there is an increase in the thermal load. However, a change in the slope of COP's curve is noticeable for values of $\dot{Q}_{GEN}$ greater than 4.00 kW, which indicates the tendency of a reversal of behavior, i.e., it is suggested that there will be a value of $\dot{Q}_{GEN}$ in which this Coefficient of Performance will start to reduce. Regardless of whether the Coefficient of Performance value is calculated by Eq. (03) or Eq. (07), the COP value will be very close to each other, presenting a 0.021%, maximum relative error between them, as expected because it is being analyzed on a steady state. Table 03 shows the information about COP_{VCC}, COP_{SYSTEM} and the relative error between them for the various thermal load values.

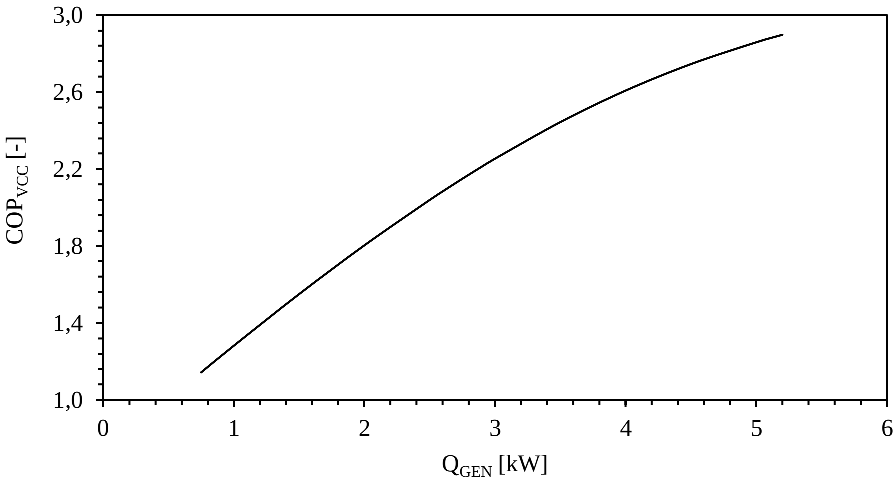

Figure 05. Variation of COP related to intensity of Thermal Load.

Table 03. COP and Relative Error for several Thermal Load values on Refrigerated Space.

$\dot{Q}_{GEN}$ **[kW]**	COP_{VCC} **[-]**	COP_{SYSTEM} **[-]**	**Relative Error [%]**
0.75	1.1425	1.1423	0.021%
1.00	1.2811	1.2814	0.021%
1.50	1.5494	1.5495	0.008%
2.00	1.8032	1.8034	0.010%
2.50	2.0392	2.0392	0.000%
2.60	2.0839	2.0841	0.012%
2.70	2.1278	2.1280	0.010%
2.80	2.1707	2.1708	0.006%
2.90	2.2127	2.2126	0.004%
3.00	2.2537	2.2538	0.006%
3.50	2.4439	2.4441	0.008%
4.00	2.6078	2.6078	0.002%
4.50	2.7455	2.7456	0.005%
5.00	2.8588	2.8585	0.010%
5.20	2.8979	2.8981	0.006%

Figure 06 shows that there is an increase in the second law efficiency up to a specific thermal load value and after this, the η_{II} tends to decrease, suggesting that there is an ideal thermal load value to be installed in the refrigerated space in order to present the highest second law efficiency. In this case, the maximum value of η_{II} was 10.64% when the thermal load was 2.70 kW. This thermal load value refers to the design limit of the refrigeration system to present a good efficiency. Physically, it would be the operating condition in which the system has the best capacity to remove heat from the refrigerated space through the evaporator, directing the system to a better refrigerating effect and making use of less energy consumption for the VCC operation. In terms of exergy discuss, it can be said that it is the region in which the system manages to transform a large part of the available exergy to obtain the refrigerating effect. It is important to emphasize that, above 5.20 kW, there is no coherent physical response, as a negative value was obtained for the second law efficiency.

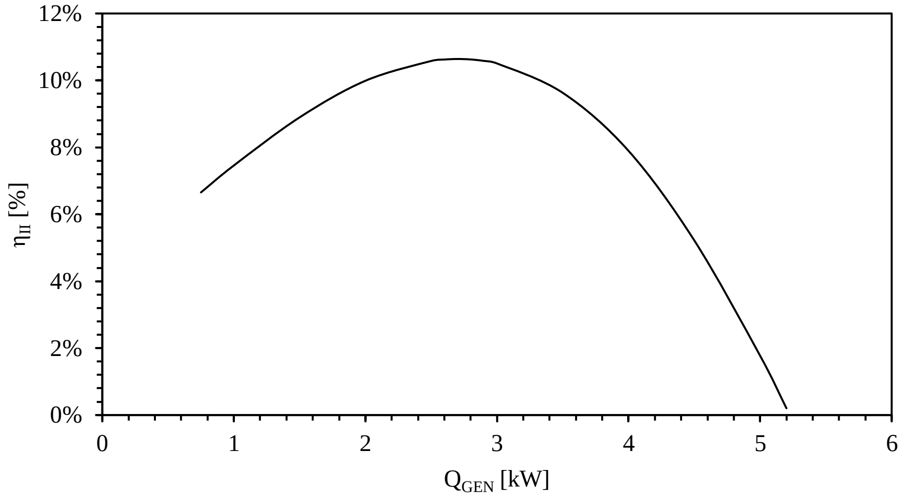

Figure 06. Variation of the Second Law Efficiency related to intensity of Thermal Load.

By treating the compressor power as an input parameter for the model, as mentioned in Section 2.1.1, the pressures of the refrigerant fluid that is flowing through the heat exchangers could be determined. Assuming a pressure ratio (p_R) of 6 between the condenser and the evaporator pressures, it is estimated, for these simulation conditions presented in this study, that the evaporator pressure is approximately 222.46 kPa, while the condenser pressure is estimated in 1334.76 kPa.

4. CONCLUSION

- This Paper presented a mathematical model developed through the application of mass and energy conservation laws for the simulation of a Vapor Compression Cycle (VCC) in steady state, as well as an equation to observe the behavior of the air temperature in the refrigerated space in transient regime coupled to a refrigeration system modeled by VCC, characterizing a *quasi*-steady state analysis.
- An exergy analysis of VCC was proposed in order to estimate the second law efficiency.
- For the numerical solution conducted in FORTRAN® 95, R22 was used as the refrigerant fluid and the compressor was submitted by 15 different thermal loads.
- The air temperature is reduced over time with greater intensity, the lower the thermal load present in the refrigerated space (RS), until reaching the steady state. The higher the thermal load in RS, the higher the air temperature will be for a constant value of compressor power.
- For thermal load values between 0.75 kW and 5.20 kW, an increase in the Coefficient of Performance (COP) with the increase in the thermal load, but with a reduction in the slope of the curve for $\dot{Q}_{GEN}$ values greater than 4.00 kW was observed, raising the hypothesis of a reduction in Coefficient of Performance after a specific thermal load condition.
- The thermal load proved to be an analysis parameter that enables reaching a maximum value for the second law efficiency of VCC.
- Through the model presented in this study, it was possible to estimate the pressure level in each of the heat exchangers that make up the VCC (i.e., evaporator and condenser), keeping the compressor power value constant.

5. ACKNOWLEDGEMENTS

The authors of this study are grateful to the Brazilian National Council of Scientific and Technological Development, CNPq (Projects 407198/2013-0, 403560/2013-6, 407204/2013-0, 430986/2016-5, 443823/2018-9, 313646/2020-1, 310708/2017-6, 308460/2020-0 and 446787/2020-5), CAPES, Ministry of Education, Brazil (Projects 062/14 and CAPES-PRINT-UFPR-88881.311981/2018-01), and Araucária Foundation of Paraná, Brazil (Projects 115/2018, N. 50.579 – PRONEX).

6. REFERENCES

Brasil. MME – Ministério de Minas e Energia. *Balanço Energético Nacional 2021: Ano Base 2020*, 2021. Available online on website: https://www.epe.gov.br/pt/publicacoes-dados-abertos/publicacoes/balanco-energetico-nacional-2021. Accessed on August 27, 2021.

Hermes, C. J. L. *Heat Transfer and Pressure Drop Trade-Offs in Liquid-to-Suction Heat Exchangers*. International Journal of Refrigeration, 2019.

Hu, Bin; Wu, Di; Wang, R. Z. *Water Vapor Compression HVAC-R Systems and its Various Applications*. Renewable and Sustainable Energy Reviews, v. 98, p. 92-107, 2018.

Jung, Wooyoung; Jazizadeh, Farrokh. *Human-in-the-loop HVAC Operations: A Quantitative Review on Occupancy, Comfort, and Energy-efficiency Dimensions*. Applied Energy, v. 239, p. 1471-1508, 2019.

Nunes, T. K. et al. *Modeling, Simulation and Optimization of a Vapor Compression Refrigeration System Dynamic and Steady state Response*. Applied Energy, v. 158, p. 540-555, 2015.

Rismanchi, Behzad et al. *Control Strategies in Multi-Zone Air Conditioning Systems*. Energies, v. 12, n. 3, p. 347, 2019.

Shahrestani, Mehdi et al. *Decision-making on HVAC&R Systems Selection: A Critical Review*. Intelligent Buildings International, v. 10, n. 3, p. 133-153, 2018.

Wang, F. Q. et al. *A Novel Special Distributed Method for Dynamic Refrigeration System Simulation*. International Journal of Refrigeration, v. 30, n. 5, p. 887-903, 2007.

Yang, S.; Ordoñez, J. C.; Vargas, J. V. C. *Constructal Vapor Compression Refrigeration (VCR) Systems Design*. International Journal of Heat and Mass Transfer, v. 115, p. 754-768, 2017.

Yang, Min-Hsiung; Yeh, Rong-Hua. *Performance and Exergy Destruction Analyses of Optimal Subcooling for Vapor-Compression Refrigeration Systems*. International Journal of Heat and Mass Transfer, Volume 87, Pages from 1 to 10, 2015.

Zubair, Syed M. et al. *Thermodynamic Optimization of Finite Time Vapor Compression Refrigeration Systems*. Energy Conversion and Management, v. 42, n. 12, p. 1457-1475, 2001.

7. RESPONSIBILITY NOTICE

The authors are the only responsible for the printed material included in this Paper.